J. Cent. South Univ. (2022) 29: 1262−1273
DOI: https://doi.org/10.1007/s11771-022-4971-3

Springer

Experimental investigation on synergetic prediction of granite rockburst using rock failure time and acoustic emission energy

WANG Chun-lai(王春来)[1]*, CAO Cong(曹聪)[1], LI Chang-feng(李长峰)[1],
CHUAI Xiao-sheng(揣筱升)[1]*, ZHAO Guang-ming(赵光明)[2], LU Hui(卢辉)[3]

1. School of Energy and Mining Engineering, China University of Mining and Technology Beijing, Beijing 100083, China;
2. School of Energy and Safety Engineering, Anhui University of Science and Technology, Huainan 232001, China;
3. Center for Underground Construction and Tunnelling, Colorado School of Mines, Golden, Colorado 80401, USA

Abstract: The frequent occurrence of rockburst and the difficulty in predicting were considered in deep engineering and underground engineering. In this work, laboratory experiments on rockburst under true triaxial conditions were carried out with granite samples. Combined with the deformation characteristics of granite, acoustic emission (AE) technology was well applied in revealing the evolution law of micro-cracks in the process of rockburst. Based on the comprehensive analysis of acoustic emission parameters such as impact, ringing and energy, the phased characteristics of crack propagation and damage evolution in granite were obtained, which were consistent with the stages of rock deformation and failure. Subsequently, based on the critical point theory, the accelerated release characteristics of acoustic emission energy during rockburst were analyzed. Based on the damage theory, the damage evolution model of rock under different loading conditions was proposed, and the prediction interval of rock failure time was ascertained concurrently. Finally, regarding damage as an intermediate variable, the synergetic prediction model of rock failure time was constructed. The feasibility and validity of model were verified.

Key words: rockburst; acoustic emission energy; damage; failure time; synergetic prediction

Cite this article as: WANG Chun-lai, CAO Cong, LI Chang-feng, CHUAI Xiao-sheng, ZHAO Guang-ming, LU Hui. Experimental investigation on synergetic prediction of granite rockburst using rock failure time and acoustic emission energy [J]. Journal of Central South University, 2022, 29(4): 1262 − 1273. DOI: https://doi. org/10.1007/s11771-022-4971-3.

1 Introduction

The deeper the mining depth of underground engineering, the greater the probability of mine disasters with the influence of complicated environment. Affected by engineering disturbances during the production process, local areas in deep engineering exhibit a high stress state. Accompanied by the rapid release of a large amount of elastic

Foundation item: Projects(52074294, 51574246, 51674008) supported by the National Natural Science Foundation of China; Projects (2017YFC0804201, 2017YFC0603000) supported by the National Key Research and Development Program of China; Project(2011QZ01) supported by the Fundamental Research Funds for the Central Universities, China
Received date: 2020-10-15; **Accepted date:** 2021-05-07
Corresponding author: WANG Chun-lai, PhD, Professor; Tel: +86-13811322376; E-mail: clwang@cumtb.edu.cn; ORCID: https://orcid.org/0000-0003-4935-4945; CHUAI Xiao-sheng, PhD, Associate Research Fellow; Tel: +86-13683081056; E-mail: chuaixiaosheng@126.com; ORCID: https://orcid.org/0000-0003-2438-3758

strain energy, a rockburst disaster occurs along with severe damage [1 − 4]. Rockburst, which has the characteristics of violent destruction, releasing large amounts of energy and being unpredictable, mostly occurs in hard-brittle rocks, such as granite, marble, and sandstone [5]. This disaster can cause damage to equipment, casualties, and partial collapse of roadways. Obviously, it has a profound impact on the safety and efficient development of deep engineering [6, 7]. The recent years have witnessed that more and more scholars pay special attention to rockburst [8]. Investigating rockburst mechanisms and predicting rockburst has become important research topics in existing research [9, 10].

Acoustic emission (AE) is an associated phenomenon that occurs in the process of rock deformation and failure, and its data contain information about the internal structural changes of rocks [11−13]. As a non-destructive testing method, AE technology has been well applied in the field of rockburst monitoring and prediction [14, 15]. Based on AE tests, the relative quiet period of AE was defined as the precursor of rock failure under uniaxial loading [16, 17]. The AE signal information was found to be consistent with the fracture damage evolution process of rock materials through AE tests and EME tests [18]. The laboratory test on samples with rockburst tendency showed that the lower the AE frequency, the higher the corresponding energy and the more severe the rockburst [19, 20]. Combined with the evolution characteristics of AE energy of granite, the relationship between AE characteristics and actual rockburst events was investigated to propose an AE-based rockburst criterion [21−23].

Nowadays, the prediction and evaluation of rock failure time are mainly based on damage theory, load−unload response ratio theory, catastrophe theory and accelerated energy release theory. Many scholars have conducted extensive research and presented many results. Based on the Murakami-Ohno creep damage theory, the basic damage relationship of jointed rock mass was derived and the meso-scale initial damage tensor was calculated [24 − 27]. The grey cusp catastrophe model of AE parameters [28] was established by using grey theory and catastrophe theory, and the identification and prediction of rockburst can be realized through the AE mechanism of the stress loading process. Based on seismic dynamics theory, the Omori-Utsu power pattern model for time series was obtained by cyclic loading AE tests [29]. The processes and precursory characteristics of a series of earthquakes were researched based on the theory of loading-unloading response ratio [30, 31], which provided a new prediction assessment method for earthquakes. By analyzing the power-law relationship between the number of AE events and the failure time, an evaluation method for rock instability was obtained [32]. The characteristics of AE event rate at unstable crack propagation stage were investigated and the interevent time (IET) function $F(\tau)$ was adopted to interpret the AE time-series from damage to ultimate failure [33]. Based on the theory of accelerated energy release, the failure time method was well applied to earthquake prediction in Taiwan, China and the accelerated energy release model was obtained to research the seismic activity [34].

However, the above-mentioned research only used AE technology to qualitatively analyze the precursory characteristics of rockburst and the process of internal crack propagation. Few attentions were paid to the coupling relationship between mechanical parameters, AE parameters and failure time in rockburst. Therefore, the AE characteristics of granite under true triaxial loading−unloading conditions were analyzed by AE experiments. Moreover, based on the critical point theory, the evolution law of AE energy and the precursory information of rockburst were analyzed. Based on the damage theory, a synergistic prediction model of rock failure time was constructed to improve the accuracy of rockburst prediction.

2 Materials and methods

2.1 Experimental materials

Rock samples were collected from the quarry in Lingshou County, Shijiazhuang City, Hebei Province, China. The materials were natural water-bearing granite, obtained from the same rock mass. Before experiments, these granite samples were processed into standard square specimens with size of 100 mm×100 mm×100 mm and 150 mm×150 mm×150 mm, and were divided into A and B groups. To improve the accuracy of experiment results, the

specimens were polished to obtain parallelism less than 0.05 mm and the vertical direction accuracy less than 0.25° . The physical and mechanical parameters of granite samples are shown in Table 1.

2.2 Experimental equipment

True triaxial compression tests were carried out on the rock mechanics servo testing machine. Meanwhile, a PCI-II full-digital AE system manufactured by the PAC company was used to monitor and collect AE signals in the whole process. The AEwin software with hit-based mode was used for the acquisition of AE parameters [35, 36]. The sampling frequency was 1 MHz and the preamplifier parameter was 40 dB [37, 38]. Specific parameter setting and preliminary preparation of the experimental can be referred to Ref. [39].

2.3 Experimental methods

During the experiment, the loading system and the AE monitoring system were always carried out synchronously. Through the loading control methods, three directions were loaded at the same time. The loading path is shown in Figure 1(a). In stage I, a set of pressure thresholds were set to simulate the in-situ stress where the specimens were located. We simplified the in-situ stress state by setting σ_1 to 15 MPa, σ_2 to 10 MPa and σ_3 to 5 MPa, according to the field stress test. The loading rates of σ_1, σ_2 and σ_3 were set to 300, 200, and 100 N/s, respectively. In stage II, when σ_1, σ_2 and σ_3 were simultaneously reached the in-situ stress, σ_3 was suddenly released and the stress was maintained in all three directions. In stage III, the maintained stress σ_2 was constant. In order to better simulate rockburst, the loading rate of σ_1 was set to 2000 N/s until the rock failed. The loading direction and AE sensors layout are shown in Figure 1(b).

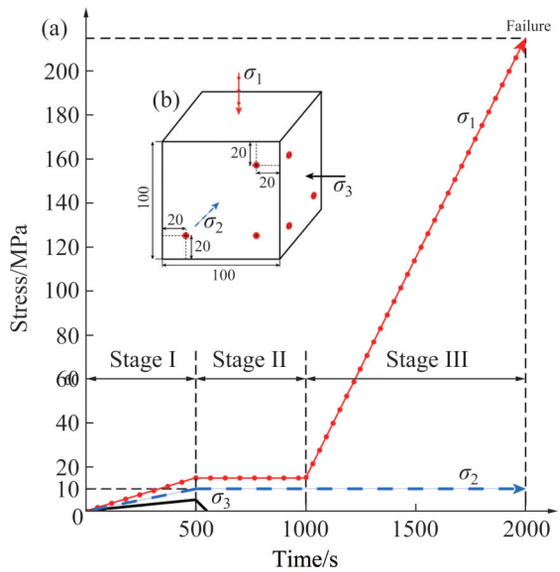

Figure 1 Experimental methods: (a) Loading path; (b) AE sensors layout (Length unit: mm)

3 Theory basis

3.1 Accelerated release model of AE energy

Many scholars have conducted a lot of research on the phenomenon of accelerated release of seismic activity. Among them, the failure time has become an important method to quantitatively describe the seismicity before earthquakes. Based on crack propagation and damage mechanics models, the accelerated release model of seismicity

Table 1 Physic-mechanical parameters of granite samples

No.	Length/mm	Width/mm	Height/mm	Mass/g	Density/(g·cm^{-3})	σ_1/MPa
A1	101.07	100.43	103.51	2941.00	2.80	189.05
A2	103.89	100.50	100.70	2955.00	2.81	178.18
A3	104.07	100.55	100.52	2966.00	2.82	222.18
A4	100.80	100.64	103.41	2939.50	2.80	232.99
A5	100.33	100.61	103.12	2930.00	2.82	239.17
A6	102.46	101.21	100.09	2893.00	2.79	189.79
B1	154.17	155.39	154.45	10420.00	2.82	197.36
B2	152.66	155.85	155.17	10425.00	2.82	197.37
B3	153.69	154.83	154.47	10432.00	2.84	193.93
B4	153.28	155.31	154.83	10445.00	2.83	194.50
B5	152.99	153.74	155.45	10386.00	2.84	195.75

was derived, which could be expressed as [40−42]:

$$(\sum \Omega)\, t = A + B\left(t_{\mathrm{f}} - t\right)^{z} \tag{1}$$

where Ω is the measurement parameter of seismic activity, t_{f} is the failure time, A and B are constants, and z is the critical exponent.

Under true triaxial conditions, the internal crack propagation of rock is greatly similar to those during natural earthquakes. And AE events caused by rock microcracks could be regarded as small-scale earthquakes. Therefore, based on the critical point theory, AE energy was used to investigate the accelerated release process of AE signals before rockburst. The accumulated AE energy W and time t were substituted into Eq. (1), and the accelerated release model of AE energy could be expressed as follows:

$$W = A + B\left(t_{\mathrm{f}} - t\right)^{z} \tag{2}$$

3.2 Synergetic prediction model of rock failure time

3.2.1 Synergetic prediction model under equal-loading conditions

Based on the generalized Hooke model and the hypothesis of strain equivalence [43], the damage constitutive relation of rock was constructed as follows:

$$[\sigma] = [\sigma^{*}](I - D) = [C][\varepsilon](1 - D) \tag{3}$$

where σ is the stress, σ^{*} is the effective stress, I is the identity matrix; D is the damage variable and ε is the strain.

Substituting σ_1, σ_2, and σ_3 into Eq. (3), the damage constitutive relation of rock under triaxial conditions could be expressed as follows:

$$\sigma_1 = E_0\varepsilon_1(1 - D) + \mu\left(\sigma_2 + \sigma_3\right) \tag{4}$$

where E_0 is the elastic modulus, ε_1 is the axial strain, and μ is Poisson ratio.

The damage evolution of rock follows the statistical distribution of Weibull [44]. Thus,

$$D(t) = 1 - \frac{N(t)}{N_0} \tag{5}$$

where $D(t)$ is the damage variable at time t; $N(t)$ is the number of micro-units that were not destroyed at time t; and N_0 is the total number of internal micro-units in rock.

The applied stress under equal-loading conditions changed linearly with time, as follows:

$$\sigma(t) = kt \tag{6}$$

where $\sigma(t)$ is the stress applied to rock at time t; k is the loading rate.

Substituting Eqs. (5) and (6) into Eq. (3), the effective stress was as follows:

$$\sigma^{*}(t) = \frac{N_0}{N(t)}kt \tag{7}$$

where $\sigma^{*}(t)$ is the time-dependent effective stress.

Based on the definition [45], the failure rate could be expressed as follows:

$$v(t) = \frac{\left[N_0 - N(t)\right]'}{N(t)} \tag{8}$$

where $v(t)$ is the failure rate of rock.

The power-law relation between the failure rate and the effective stress in the process of rock failure was proposed by COLEMAN [45]:

$$v(t) = v_{\mathrm{f}}\left[\frac{\sigma^{*}(t)}{\sigma\left(t_{\mathrm{f}}\right)}\right]^{\rho} \tag{9}$$

where $\sigma\left(t_{\mathrm{f}}\right)$ is the applied stress of rock failure; v_{f} is the failure rate in the process of rock failure; and ρ is the failure index of rock.

Substituting Eqs. (6) and (7) into Eq. (9), the failure rate of rock could be expressed as follows:

$$v(t) = v_{\mathrm{f}}\left[\frac{N_0 t}{N(t)t_{\mathrm{f}}}\right]^{\rho} \tag{10}$$

Then, Eq. (5) and Eq. (8) were substituted into Eq. (10), and the damage evolution model of rock was as follows:

$$D(t) = 1 - \left[1 - \left(\frac{t}{t_{\mathrm{f}}}\right)^{\rho+1}\right]^{\frac{1}{\rho}} \tag{11}$$

Through the research, the relationship between the principal strain and the loading time could be determined as follows:

$$\varepsilon(t) = A_1\exp\left(B_1 t\right) + \varepsilon_0 \tag{12}$$

where A_1, B_1, and ε_0 are constants, which could be determined by fitting curve.

Substituting Eqs. (11) and (12) into Eq. (4), the

damage constitutive equation of rock could be expressed as follows:

$$\sigma_1 = E_0\left[A_1\exp\left(B_1 t\right)+\varepsilon_0\right]\left[1-\left(\frac{t}{t_\mathrm{f}}\right)^{\rho+1}\right]^{\frac{1}{\rho}}+\mu\left(\sigma_2+\sigma_3\right) \tag{13}$$

Combined with the above analysis, a synergetic prediction model of rock failure time under equal-loading conditions was constructed as follows:

$$\begin{cases}\sigma_1(t) = E_0\left[A_1\exp\left(B_1 t\right)+\varepsilon_0\right]\left[1-\left(\frac{t}{t_\mathrm{f}}\right)^{\rho+1}\right]^{\frac{1}{\rho}}+\mu\left(\sigma_2+\sigma_3\right)\\ D(t) = 1-\left[1-\left(\frac{t}{t_\mathrm{f}}\right)^{\rho+1}\right]^{\frac{1}{\rho}}\\ W(t) = A+B\left(t_\mathrm{f}-t\right)^z\end{cases} \tag{14}$$

3.2.2 Synergetic prediction model under equal-displacement conditions

In the research of rock damage evolution, rocks were considered frequently to be composed of multiple micro-units. In this paper, it was assumed that the intensity of micro-units in rock conforms to the Weibull distribution, and its probability density could be expressed as follows:

$$\Phi(F) = \frac{m}{F_0}\left(\frac{F}{F_0}\right)^{m-1}\exp\left[-\left(\frac{F}{F_0}\right)^m\right] \tag{15}$$

where F_0 is the Weibull distribution parameter of micro-units' intensity, and m is the degree of non-uniformity of Weibull distribution.

Therefore, the destroyed number of micro-units could be expressed as follows:

$$N_F = \int_0^F N_0\Phi(F)\,\mathrm{d}F = N\left\{1-\exp\left[-\left(\frac{F}{F_0}\right)^m\right]\right\} \tag{16}$$

where N_F is the destroyed number of micro-units, N_0 is the total number of micro-units.

In this paper, the axial principal strain ε_1 was used to represent the intensity of micro-units F. Therefore, the damage variable D was as follows:

$$D = \frac{N_\mathrm{f}}{N_0} = 1-\exp\left[-\left(\frac{\varepsilon_1}{\alpha}\right)^m\right] \tag{17}$$

where α is the relative parameter of rock.

Substituting Eq. (17) into Eq. (4), the statistical damage constitutive relation of crack propagation under triaxial loading conditions could be expressed as follows:

$$\sigma_1 = E_0\varepsilon_1\exp\left[-\left(\frac{\varepsilon_1}{\alpha}\right)^m\right]+\mu\left(\sigma_2+\sigma_3\right) \tag{18}$$

The relationship between the axial strain and time series under equal-displacement conditions was as follows:

$$\varepsilon(t) = \dot{\varepsilon}t+\varepsilon_0 \tag{19}$$

where $\dot{\varepsilon}$ is strain rate and ε_0 is the initial axial strain.

Substituting Eq. (19) into Eq. (17), the damage evolution of rock could be expressed as follows:

$$D(t) = 1-\exp\left[-\left(\frac{\dot{\varepsilon}t+\varepsilon_0}{\alpha}\right)^m\right] \tag{20}$$

Substituting Eq. (19) into Eq. (18), the damage constitutive equation of time variable could be expressed as follows:

$$\sigma_1 = E_0\left(\dot{\varepsilon}t+\varepsilon_0\right)\exp\left[-\left(\frac{\dot{\varepsilon}t+\varepsilon_0}{\alpha}\right)^m\right]+\mu\left(\sigma_2+\sigma_3\right) \tag{21}$$

Combined with Eq. (2), a synergetic prediction model of rock failure time under equal-displacement conditions was constructed as follows:

$$\begin{cases}\sigma_1(t) = E_0\left(\dot{\varepsilon}t+\varepsilon_0\right)\exp\left[-\left(\frac{\dot{\varepsilon}t+\varepsilon_0}{\alpha}\right)^m\right]+\mu\left(\sigma_2+\sigma_3\right)\\ D(t) = 1-\exp\left[-\left(\frac{\dot{\varepsilon}t+\varepsilon_0}{\alpha}\right)^m\right]\\ W(t) = A+B\left(t_\mathrm{f}-t\right)^z\end{cases} \tag{22}$$

4 Results

The AE monitoring system was used to obtain the data of AE characteristic parameters related to rockburst under true triaxial conditions, such as the count of impact, ringing, and energy. As shown in Figures 2 and 3, the AE time series characteristics of typical granite samples were indicated.

The time series characteristics of AE parameters of sample A3 are shown in Figure 2. In stages I and II, only small amounts of AE signals

were generated due to the gradual closure of the original cracks inside the rock. Part of AE signals were generated during the beginning and end of stage II, but in general, the cumulative value of AE parameters did not change significantly. In stage III, AE activities were relatively rare near the peak stress of 7%−56%, and the values of AE parameters remained unchanged. The AE events were relatively active near the peak stress of 56% − 89%. In this stage, the internal cracks of rock propagated steadily under the action of stress. Near the peak stress of 89% − 100%, large number of cracks expanded and penetrated into a rupture zone, and the macroscopic failure was eventually formed. In the meantime, the AE energy was released at a fast rate and reached the maximum value in an extremely short time near the peak stress. And then, the stress and the AE energy decreased sharply.

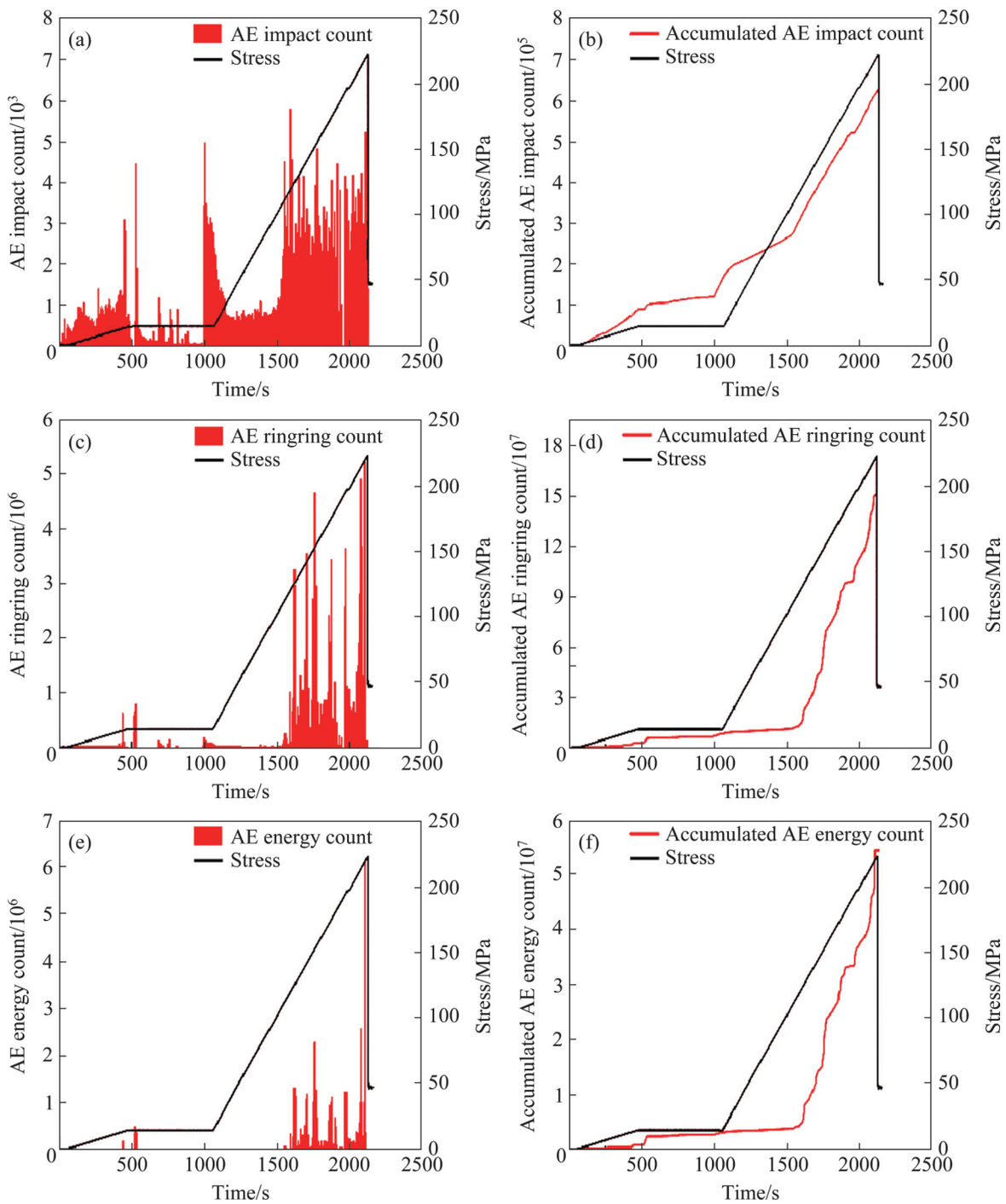

Figure 2 AE characteristics of granite sample A3: (a) AE impact count; (b) Accumulated AE impact count; (c) AE ringing count; (d) Accumulated AE ringing count; (e) AE energy count; (f) Accumulated AE energy count

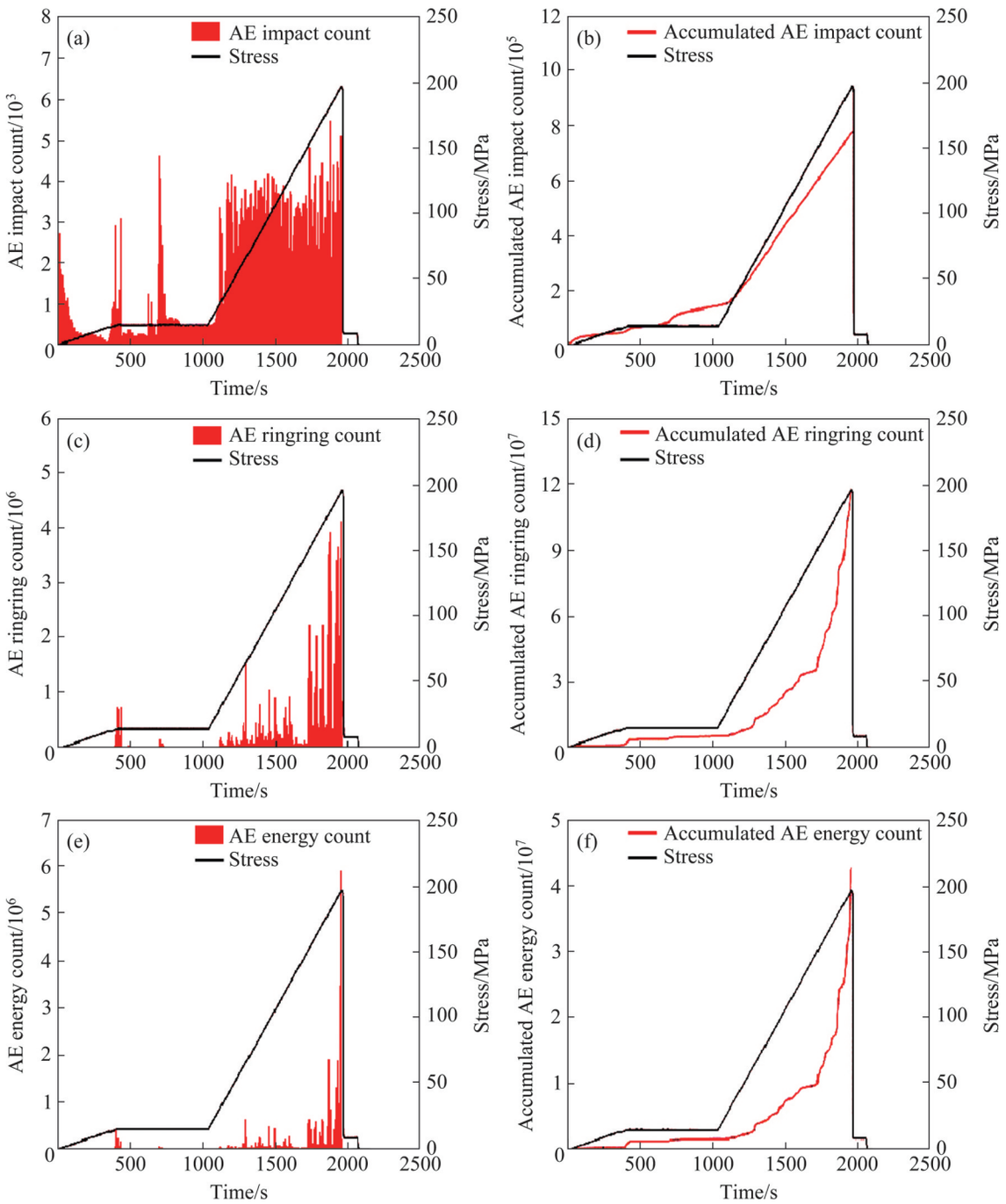

Figure 3 AE characteristics of granite sample B2: (a)AE impact count; (b) Accumulated AE impact count; (c) AE ringing count; (d) Accumulated AE ringing count; (e)AE energy count; (f) Accumulated AE energy count

5 Analysis and discussion

5.1 Accelerated release characteristics of AE energy

According to Eq. (2), the release process of AE energy during rockburst was fitted by the power-law relationship. The fitting curve and the nonlinear regression equation of AE energy are shown in Figure 4. Meanwhile, the fitting parameters are shown in Table 2. Obviously, the parameters z and r, which represent the accelerated release process of AE energy, are less than 1, and the critical exponents z of A1, A4 and A5 are all less than 0.2. It shows obviously that AE energy has an accelerated release characteristic in the process of rockburst. This conclusion was consistent with the previous results of the z-value range of seismic data [23].

Combined with high-speed camera technology, the accelerated release process of AE energy was analyzed. In the initial loading stage, the release rate of AE energy was relatively low due to the slow development of cracks in rock, and there was no obvious accelerated release phenomenon. With the increase of load stress, new cracks were generated and AE energy increased gradually. In the vicinity of the peak stress, the release rate of AE energy increased rapidly and reached the maximum value in an extremely short time. Therefore, the accelerated release characteristics of AE energy could be used as the precursor information for rockburst prediction.

5.2 Verification of synergetic prediction model of rock failure time

5.2.1 Verification under equal-loading conditions

The synergetic prediction model of rock failure time Eq. (14) was verified by sample A3. The basic mechanical parameters are as follows: E_0=81.20 GPa, μ=0.18, σ_2=10 MPa and σ_3=5 MPa.

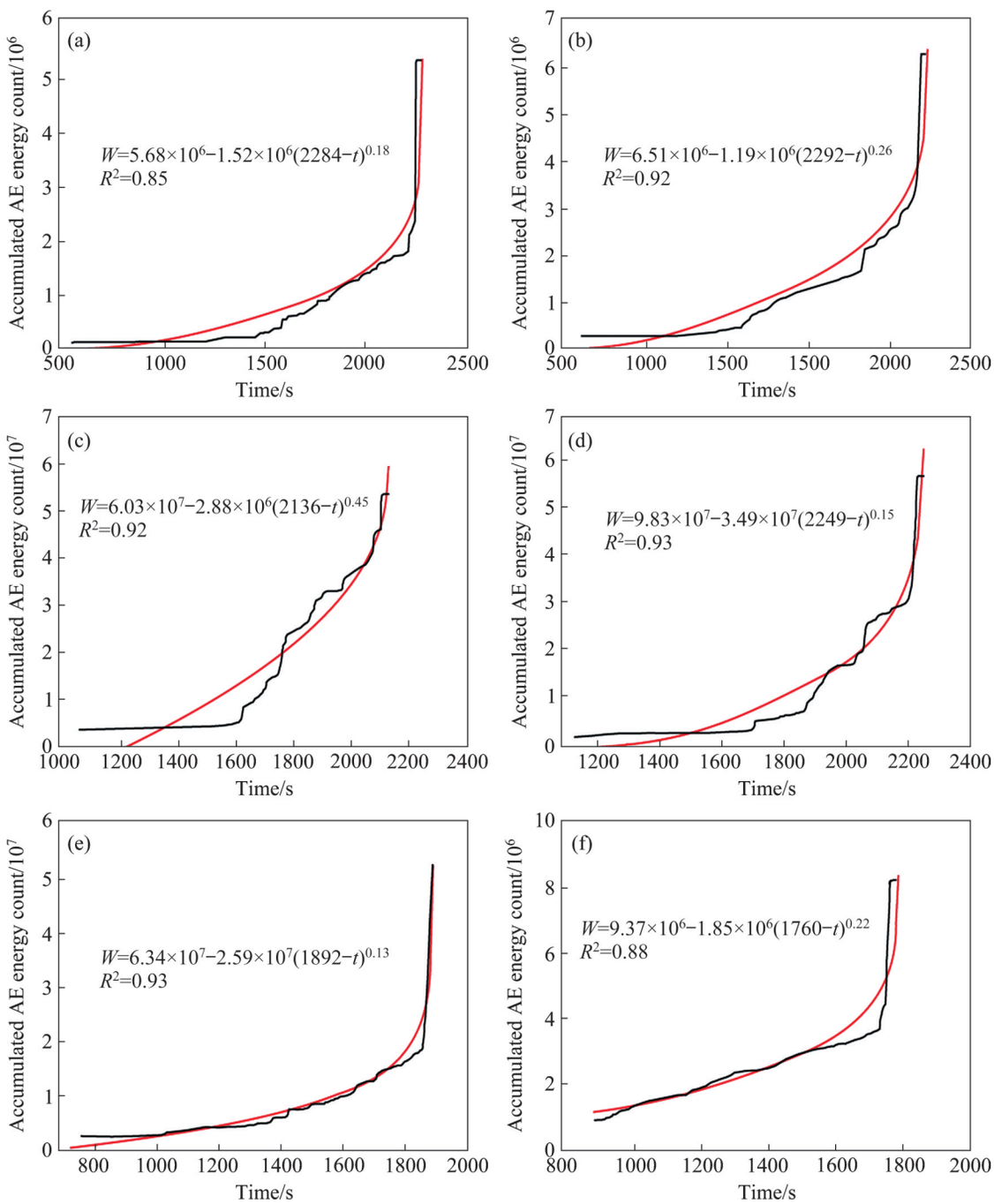

Figure 4 Fitting curve of relationship between AE energy and time: (a) A1; (b) A2; (c) A3; (d) A4; (e) A5; (f) A6

Table 2 Fitting parameters of AE cumulative energy

No.	R^2	$A/10^6$	$B/10^6$	t_f/s	z	r
A1	0.85	5.68	−1.52	2284	0.18	0.21
A2	0.92	6.51	−1.19	2292	0.26	0.31
A3	0.92	60.3	−2.88	2136	0.45	0.36
A4	0.93	98.3	−34.9	2249	0.15	0.13
A5	0.93	63.4	−25.9	1892	0.13	0.28
A6	0.88	9.37	−1.85	1760	0.22	0.30

1) Calculating the parameters A_1, B_1 and ε_0. As shown in Figure 5, the fitting curve of strain−time was obtained by Eq. (12). The values of the fitting parameters are A_1=1.02×10^{-5}, B_1=1.44×10^{-3}, and ε_0=0.0097.

2) Calculating the parameters ρ and t_f. As shown in Figure 6, the damage variable was fitted by Eq. (11), and the fitting parameters are ρ=0.27 and t_f=2136.

3) Verification. The experimental parameters of the synergistic prediction model under equal-loading conditions are shown in Table 3. Substituting the peak principal stress into Eq. (14), the failure time of sample A3 was calculated to be 2124.56 s. In addition, the failure time of sample A3 calculated by Eq. (2) was 2136.16 s. Therefore, the failure time interval of rock obtained by the synergetic prediction model was 2124.56−2136.16 s, which included the actual failure time of 2136.00 s. To sum up, this synergetic model can effectively predict rockburst disasters under equal-load conditions.

5.2.2 Verification under equal-displacement conditions

The synergetic prediction model of rock failure time Eq. (22) was verified by sample F2 at a loading rate of 0.002 mm/s. The basic mechanical parameters are as follows: E_0=61.10 GPa, μ=0.17, σ_2=σ_3=0 MPa.

1) Calculate the parameters ε_0, m and F_0. The experimental parameters are ε_0=0.00018, m =8.24, and F_0=16.14.

2) Calculate the parameter t_f. As shown in Figure 7, the AE energy of sample F2 was fitted by the acceleration release model Eq. (2). According to the fitting curve, the failure time of rock is 938 s.

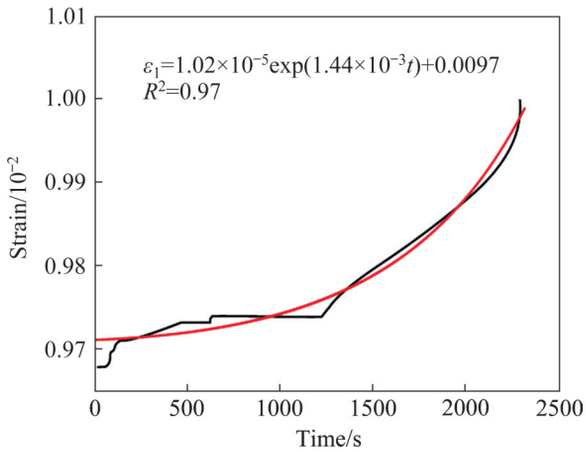

Figure 5 Fitting curve of strain-time

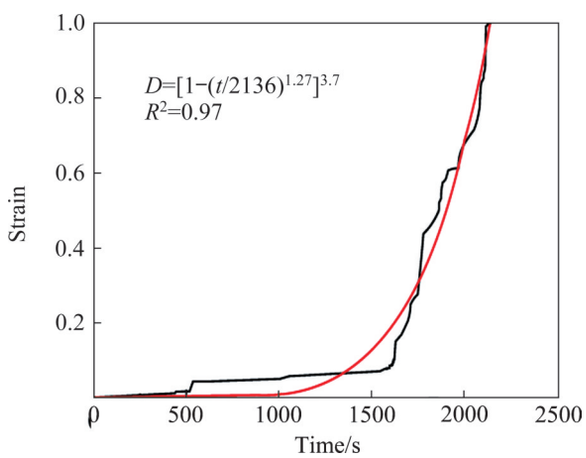

Figure 6 Fitting curve of damage-time

3) Verification. The experimental parameters of the synergetic prediction model under equal-displacement conditions are shown in Table 4. Substituting the peak principal stress into Eq. (22), the failure time of sample F2 was calculated to be 924.38 s. Therefore, the failure time interval of rock obtained by the synergetic prediction model was 924.38−938 s, which included the actual failure time of 931.60 s.

In summary, the rock failure time calculated by the synergistic prediction model is greatly similar to the actual failure time. It is indicated that the synergistic prediction model of rock failure time could provide theoretical guidance for rockburst

Table 3 Experimental parameters of synergetic prediction model under equal-loading conditions

Specimen	Mechanical parameter				Fitting parameter				
	σ_2/MPa	σ_3/MPa	E_0/MPa	μ	$A_1/10^{-5}$	$B_1/10^{-3}$	ε_0	ρ	t_f/s
A3	10	5	81,200	0.24	1.02	1.44	0.0097	0.27	2136

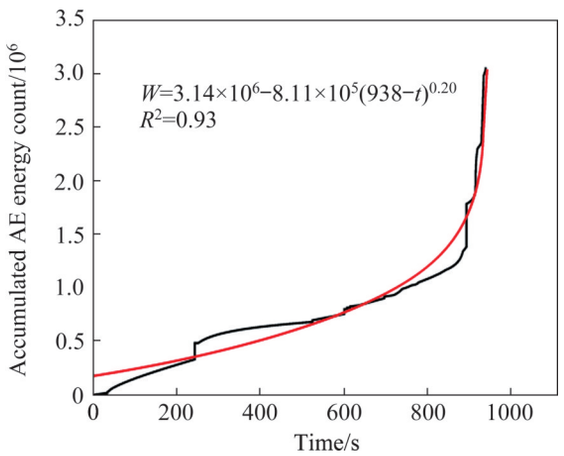

Figure 7 Fitting curve of AE energy of sample F2

Table 4 Experimental parameters of synergetic prediction model under equal-displacement conditions

Specimen	Mechanical parameter				Test parameter		
	σ_2/MPa	σ_3/MPa	E_0/MPa	μ	ε_0	m	F_0
F2	0	0	61100	0.17	0.00018	8.24	16.14

prediction. Moreover, the calculated time interval of rock failure could be used as the reference time for rockburst prediction.

6 Conclusions

Based on the experimental investigation, the AE characteristic parameters in the process of rock failure were obtained. Based on the critical point theory and damage theory, the relationship between rock failure time and different warning parameters was analyzed, and the synergistic prediction model of rock failure time was constructed preliminarily. The main conclusions can be summarized as follows:

1) The time series characteristics of AE parameters well reflect the stage characteristics of internal crack propagation and macroscopic failure of granite sample. Under true triaxial conditions, the AE energy has a relatively obvious accelerated release characteristic near the peak stress, which could be regarded as a precursory information of rockburst.

2) Based on the critical point theory, the accelerated release model of AE energy is established. Furthermore, based on the damage theory and the hypothesis of strain equivalence, the statistical damage constitutive equation of crack propagation is constructed, which explores the damage evolution process under different loading conditions.

3) Different warning parameters, such as stress, damage and AE parameters are taken into account to predict the failure time of rock, and the synergistic prediction model of failure time was preliminarily constructed. Moreover, the validity and feasibility of the model are verified by experimental data. Thus, the synergistic prediction model of rock failure time provides a meaningful method for predicting rockburst.

Contributors

WANG Chun-lai provided the idea of the study, conducted the experiments, wrote and revised the manuscript. CAO Cong wrote and revised the manuscript. LI Chang-feng analyzed the test data and modified the diagrams. CHUAI Xiao-sheng conducted the experiments. ZHAO Guang-ming and LU Hui offered some valuable suggestions for the contents of the manuscript.

Conflict of interest

WANG Chun-lai, CAO Cong, LI Chang-feng, CHUAI Xiao-sheng, ZHAO Guang-ming, and LU Hui declare that they have no conflict of interest.

References

[1] WANG Chun-lai. Evolution, monitoring and predicting models of rockburst [M]. Singapore: Springer Singapore, 2018. DOI: 10.1007/978-981-10-7548-3.

[2] COOK N G W. The failure of rock [J]. International Journal of Rock Mechanics and Mining Sciences & Geomechanics Abstracts, 1965, 2(4): 389−403. DOI: 10.1016/0148-9062(65)90004-5.

[3] KIDYBIŃSKI A. Bursting liability indices of coal [J]. International Journal of Rock Mechanics and Mining Sciences & Geomechanics Abstracts, 1981, 18(4): 295−304. DOI: 10.1016/0148-9062(81)91194-3.

[4] HOEK E, BROWN E T. Underground excavations in rock [M]. London: CRC Press, 1980.

[5] HUANG R Q, WANG X N, CHAN L S. Triaxial unloading test of rocks and its implication for rock burst [J]. Bulletin of Engineering Geology and the Environment, 2001, 60(1): 37−41. DOI: 10.1007/s100640000082.

[6] HE M C, MIAO J L, FENG J L. Rock burst process of limestone and its acoustic emission characteristics under true-triaxial unloading conditions [J]. International Journal of Rock Mechanics and Mining Sciences, 2010, 47(2): 286−298. DOI: 10.1016/j.ijrmms.2009.09.003.

[7] CAI M, KAISER P K, TASAKA Y, et al. Generalized crack

initiation and crack damage stress thresholds of brittle rock masses near underground excavations [J]. International Journal of Rock Mechanics and Mining Sciences, 2004, 41(5): 833−847. DOI: 10.1016/j.ijrmms.2004.02.001.

[8] YU Yang, CHEN Bing-rui, XU Chang-jie, et al. Analysis for microseismic energy of immediate rockbursts in deep tunnels with different excavation methods [J]. International Journal of Geomechanics, 2017, 17(5): 04016119. DOI: 10.1061/(asce)gm.1943-5622.0000805.

[9] WANG Chun-lai, CHEN Zeng, LIAO Ze-feng, et al. Experimental investigation on predicting precursory changes in entropy for dominant frequency of rockburst [J]. Journal of Central South University, 2020, 27(10): 2834−2848. DOI: 10.1007/s11771-021-4658-1.

[10] ZHOU X P, QIAN Q H, YANG H Q. Rock burst of deep circular tunnels surrounded by weakened rock mass with cracks [J]. Theoretical and Applied Fracture Mechanics, 2011, 56(2): 79−88. DOI: 10.1016/j.tafmec.2011.10.003.

[11] LOCKNER D. The role of acoustic emission in the study of rock fracture [J]. International Journal of Rock Mechanics and Mining Sciences & Geomechanics Abstracts, 1993, 30(7): 883−899. DOI: 10.1016/0148-9062(93)90041-B.

[12] KHAZAEI C, HAZZARD J, CHALATURNYK R. Damage quantification of intact rocks using acoustic emission energies recorded during uniaxial compression test and discrete element modeling [J]. Computers and Geotechnics, 2015, 67: 94−102. DOI: 10.1016/j.compgeo.2015.02.012.

[13] MORADIAN Z, EINSTEIN H H, BALLIVY G. Detection of cracking levels in brittle rocks by parametric analysis of the acoustic emission signals [J]. Rock Mechanics and Rock Engineering, 2016, 49(3): 785 − 800. DOI: 10.1007/s00603-015-0775-1.

[14] WEN Zhi-jie, WANG Xiao, CHEN Lian-jun, et al. Size effect on acoustic emission characteristics of coal-rock damage evolution [J]. Advances in Materials Science and Engineering, 2017, 2017: 3472485. DOI: 10.1155/2017/3472485.

[15] NIU Yong, ZHOU Xiao-ping, ZHOU Lun-shi. Fracture damage prediction in fissured red sandstone under uniaxial compression: Acoustic emission b-value analysis [J]. Fatigue & Fracture of Engineering Materials & Structures, 2020, 43(1): 175−190. DOI: 10.1111/ffe.13113.

[16] WANG Chun-lai, LU Hui, WANG Fu-li, et al. Characteristic point of the relatively quiet period for limestone failure under uniaxial compression [J]. Journal of Testing and Evaluation, 2015, 43(6): 20140187. DOI: 10.1520/jte20140187.

[17] SCHIAVI A, NICCOLINI G, TARIZZO P, et al. Waveforms and frequency spectra of elastic emissions due to macrofractures in solids [C]//Experimental and Applied Mechanics, 2011, 6: 613 − 621. DOI: 10.1007/978-1-4614-0222-0_73.

[18] LACIDOGNA G, CARPINTERI A, MANUELLO A, et al. Acoustic and electromagnetic emissions as precursor phenomena in failure processes [J]. Strain, 2010, 47: 144 − 152. DOI: 10.1111/j.1475-1305.2010.00750.x.

[19] LU Cai-ping, DOU Lin-ming, LIU Hui, et al. Case study on microseismic effect of coal and gas outburst process [J]. International Journal of Rock Mechanics and Mining Sciences, 2012, 53: 101 − 110. DOI: 10.1016/j.ijrmms.2012.05.009.

[20] GONG Feng-qiang, WANG Yun-liang, LUO Song. Rockburst proneness criteria for rock materials: Review and new insights [J]. Journal of Central South University, 2020, 27(10): 2793−2821. DOI: 10.1007/s11771-020-4511-y.

[21] WANG Chun-lai, BAO Tian-cai, LU Hui, et al. Variation regulation of the acoustic emission energy parameter during the failure process of granite under uniaxial compression [J]. Materials Testing, 2015, 57(9): 755 − 760. DOI: 10.3139/120.110776.

[22] ZHOU Xiao-ping, PENG Sen-lin, ZHANG Jian-zhi, et al. Predictive acoustical behavior of rockburst phenomena in Gaoligongshan tunnel, Dulong River highway, China [J]. Engineering Geology, 2018, 247: 117 − 128. DOI: 10.1016/j.enggeo.2018.10.023.

[23] BEN-ZION Y, LYAKHOVSKY V. Accelerated seismic release and related aspects of seismicity patterns on earthquake faults [J]. Pure and Applied Geophysics, 2002, 159(10): 2385−2412. DOI: 10.1007/s00024-002-8740-9.

[24] KYOYA T, KUSABUKA M, ICHIKAWA Y, et al. A damage mechanics analysis for underground excavation in jointed rock mass [C]// Proceedings of the International Symposium on Engineering in Complex Rock Formations. Amsterdam: Elsevier, 1988: 506 − 513. DOI: 10.1016/b978-0-08-035894-9.50071-8.

[25] KYOYA T, CHIKAWA Y, KAWAMOTO T. Damage mechanics theory for discontinuous rock mass [J]. International Journal of Rock Mechanics and Mining Sciences & Geomechanics Abstracts, 1987, 24(2): 52. DOI: 10.1016/0148-9062(87)91989-9.

[26] KAWAMOTO T, ICHIKAWA Y, KYOYA T. Deformation and fracturing behaviour of discontinuous rock mass and damage mechanics theory [J]. International Journal for Numerical and Analytical Methods in Geomechanics, 1988, 12(1): 1−30. DOI: 10.1002/nag.1610120102.

[27] CHIKAWA Y, KYOYA T, KAWAMOTO T. Incremental theory of plasticity for rock [J]. International Journal of Rock Mechanics and Mining Sciences & Geomechanics Abstracts, 1987, 24(2): 63. DOI: 10.1016/0148-9062(87)92079-1.

[28] LI Xing-wei. Application of working face rock burst prediction of grey modeling cusp catastrophe analysis based on the acoustic emission [J]. Applied Mechanics and Materials, 2013, 373 − 375: 689 − 693. DOI: 10.4028/www.scientific.net/amm.373-375.689.

[29] HIRATA T. Omori's Power Law aftershock sequences of microfracturing in rock fracture experiment [J]. Journal of Geophysical Research: Solid Earth, 1987, 92(B7): 6215 − 6221. DOI: 10.1029/JB092iB07p06215.

[30] YIN X C, MORA P, PENG K, et al. Load-unload response ratio and accelerating moment/energy release critical region scaling and earthquake prediction [J]. Pure and Applied Geophysics, 2002, 159(10): 2511 − 2523. DOI: 10.1007/s00024-002-8745-4.

[31] YIN Xiang-chu, LIU Yue, MORA P, et al. New progress in LURR-integrating with the dimensional method [J]. Pure and Applied Geophysics, 2013, 170(1 − 2): 229 − 236. DOI: 10.1007/s00024-012-0453-0.

[32] NISHIZAWA O, NORO H. A self-exciting process of acoustic emission occurrence in steady creep of granite under

uniaxial stress [J]. Geophysical Research Letters, 1990, 17 (10): 1521−1524. DOI: 10.1029/GL017i010p01521.
[33] ZHANG Jian-zhi, ZHOU Xiao-ping. Forecasting catastrophic rupture in brittle rocks using precursory AE time series [J]. Journal of Geophysical Research: Solid Earth, 2020, 125(8): e2019JB019276. DOI: 10.1029/2019JB019276.
[34] WANG J C, SHIEH C F. Investigation of seismicity in central Taiwan using the accelerating seismic energy release model [J]. Terrestrial, Atmospheric and Oceanic Sciences, 2004, 15(1): 1. DOI: 10.3319/tao.2004.15.1.1(t).
[35] ZHANG Jian-zhi, ZHOU Xiao-ping, ZHOU Lun-shi, et al. Progressive failure of brittle rocks with non-isometric flaws: Insights from acousto-optic-mechanical (AOM) data [J]. Fatigue & Fracture of Engineering Materials & Structures, 2019, 42(8): 1787−1802. DOI: 10.1111/ffe.13019.
[36] ZHOU Xiao-ping, ZHANG Jian-zhi, QIAN Qi-hu, et al. Experimental investigation of progressive cracking processes in granite under uniaxial loading using digital imaging and AE techniques [J]. Journal of Structural Geology, 2019, 126: 129−145. DOI: 10.1016/j.jsg.2019.06.003.
[37] ZHOU Xiao-ping, ZHANG Jian-zhi, BERTO F. Fracture analysis in brittle sandstone by digital imaging and AE techniques: Role of flaw length ratio [J]. Journal of Materials in Civil Engineering, 2020, 32(5): 04020085. DOI: 10.1061/(asce)mt.1943-5533.0003151.
[38] NIU Yong, ZHOU Xiao-ping, BERTO F. Evaluation of fracture mode classification in flawed red sandstone under uniaxial compression [J]. Theoretical and Applied Fracture Mechanics, 2020, 107: 102528. DOI: 10.1016/j.tafmec.2020.102528.
[39] WANG Chun-lai, HOU Xiao-lin, LIU Yu-bo. Three-dimensional crack recognition by unsupervised machine learning [J]. Rock Mechanics and Rock Engineering, 2021, 54(2): 893−903. DOI: 10.1007/s00603-020-02287-w.
[40] BUFE C G, VARNES D J. Predictive modeling of the seismic cycle of the Greater San Francisco Bay Region [J]. Journal of Geophysical Research: Solid Earth, 1993, 98(B6): 9871−9883. DOI: 10.1029/93JB00357.
[41] BOWMAN D D, OUILLON G, SAMMIS C G, et al. An observational test of the critical earthquake concept [J]. Journal of Geophysical Research: Solid Earth, 1998, 103(B10): 24359−24372. DOI: 10.1029/98JB00792.
[42] VERE-JONES D. Statistical theories of crack propagation [J]. Mathematical Geology, 1977, 9(5): 455－481. DOI: 10.1007/bf02100959.
[43] JEAN L. How to use damage mechanics [J]. Nuclear Engineering and Design, 1984, 80(2): 233 － 245. DOI: 10.1016/0029-5493(84)90169-9.
[44] KRAJCINOVIC D, FONSEKA G U. The continuous damage theory of brittle materials, part 1: General theory [J]. Journal of Applied Mechanics, 1981, 48(4): 809－815. DOI: 10.1115/1.3157739.
[45] COLEMAN B D. Statistics and time dependence of mechanical breakdown in fibers [J]. Journal of Applied Physics, 1958, 29(6): 968−983. DOI: 10.1063/1.1723343.

(Edited by FANG Jing-hua)

中文导读

基于岩石破裂时间与声发射能量的花岗岩岩爆协同预警试验研究

摘要：在深部岩土工程和地下工程中，岩爆等动力灾害频繁发生且难以预测。本文以花岗岩为试验对象开展真三轴岩爆室内试验研究。结合花岗岩变形特征，采用声发射(AE)技术可以很好地揭示岩爆过程中微裂纹的演化规律。对撞击计数、振铃计数和能量等声发射特征参数进行综合分析，获得了花岗岩裂纹扩展和损伤演化的阶段性特征，与岩石变形破坏过程具有较好的一致性。随后，基于临界点理论，分析了岩爆过程中声发射能量的加速释放现象。基于损伤理论，提出了不同加载条件下岩石的损伤演化模型，同时确定了岩石破裂时间的预测区间。最后，以损伤为中间变量，构建了岩石破裂时间协同预测模型，并对模型的可行性和有效性进行了验证。

关键词：岩爆；声发射能量；损伤；破裂时间；协同预警